

Superlattice Microrefrigerators Flip-Chip Bonded with Optoelectronic Devices

Yan Zhang¹, Gehong Zeng¹, Joachim Piprek², Avram Bar-Cohen³ and Ali Shakouri¹

¹ Department of Electrical Engineering, University of California – Santa Cruz, Santa Cruz, CA 95064, USA

² Electrical and Computer Engineering, University of California, Santa Barbara, CA 93106, USA

³ Department of Mechanical Engineering, University of Maryland, College Park, Maryland 2074

Corresponding contact, e-mail: ali@soe.ucsc.edu, Tel.: 831-459-1292

Abstract

A 3D electrothermal model was developed to study the InP-based thin film $\text{In}_{0.53}\text{Ga}_{0.47}\text{As}/\text{In}_{0.52}\text{Al}_{0.48}\text{As}$ superlattice microrefrigerators for various device sizes, ranging from $40 \times 40 \mu\text{m}^2$ to $120 \times 120 \mu\text{m}^2$. We discussed maximum cooling and cooling power densities for current devices, analyzed the non-idealities of current devices and proposed an optimized structure. The simulation results demonstrated a maximum cooling of 3°C with cooling power density over $300 \text{ W}/\text{cm}^2$ with an optimized structure based on the current device geometry. Furthermore, we also demonstrated that a maximum cooling, over 10°C with power density over $900 \text{ W}/\text{cm}^2$, could be possible when the current figure of merit of InGaAs/InAlAs superlattice is enhanced five times with the non-conserved lateral momentum. Besides monolithic integration, we also propose a flip-chip bonded solution to integrate these microrefrigerator with the optoelectronic chips. Preliminary 3D electrothermal simulation will be present to analyze its cooling effects for this 2-chip integration model.

Keywords

Superlattice, microrefrigerators, integration, electrothermal simulation, maximum cooling, cooling power density

Nomenclature

ZT	Figure of merit	no unit
S	Seebeck coefficient	$\mu\text{V}/\text{K}$
σ	Electrical conductivity	$(\text{ohm}\cdot\text{cm})^{-1}$
k	thermal conductivity	W/mK
ΔT	Temperature lower than ambient	K or $^\circ\text{C}$
W	Cooling power density	W/cm^2
T_{max}	Maximum cooling temperature	K or $^\circ\text{C}$
T_c	Cold side temperature	K or $^\circ\text{C}$
ΔQ	Effective interface heating/cooling power	W
I	Supplied current to microrefrigerator	mA

1. Introduction

Current trends in optoelectronic devices are to increase the speed, multi-wavelength operation and increase the level of integration. Lasers and optoelectronic devices are very sensitive to temperature. Heating in the laser's active region can reach values on the order of kW/cm^2 and the subsequent temperature rise can shift the wavelength, reduce output power and decrease the device's lifetime^[1]. The temperature dependence wavelength shift is on the order of $0.1 \text{ nm}/^\circ\text{C}$ ^[2]. The channel spacing in Wavelength-Division-Multiplexing (WDM) is only $0.2\text{--}0.4 \text{ nm}$. Thus a few degrees temperature change could result in thermal crosstalk. Currently, Bi_2Te_3

bulk thermoelectric coolers are being widely used in optoelectronics to realize temperature stabilization. However its low efficiency, low cooling power density and bulk size limit their applications^[3]. Since 1980s thermal designers have been looking for new cooling solutions that could be monolithically integrated with lasers.

In 1984, Hava et al.^[4] observed a 2°C temperature change on a GaAs/GaAlAs laser diode when it monolithically integrated with a n+ GaAs substrate thermoelectric elements at 6A current. He concluded that the benefit of improved cooling through heat spreading by metallic layer, however the additional advantage of Peltier-effect cooling is minimum because of the relatively small ratio of Seebeck coefficient to thermal conductivity for $\text{Ga}_{1-x}\text{Al}_x\text{As}$ alloys. In 1985, Dutta et al.^[5] achieved a 2.5°C temperature change on a InGaAsP laser diode when it monolithically integrated with a n-InP substrate thermoelectric elements at 50mA current. In 1991, Berger et al.^[6] reported a 7.5°C temperature change on a GaAs/AlGaAs vertical-cavity surface-emitting laser when it monolithically integrated with a n+ GaAs substrate thermoelectric elements at 100mA current. However all these results were not convincing since there is no direct temperature measurement data, the temperature changes were converted by the wavelength shift of the light emitted from the laser diode. The temperature stability of the laser and accuracy of photoluminescence characterization will both affect the temperature data. More importantly, in a three-terminal device geometry, current sent to the substrate could affect the bias condition of the laser and thus its wavelength^[7]. For example the 7.5°C temperature change reported by Berger et. al. might be inaccurate. According to the Peltier coefficient and resistivity data that they reported in the paper, we could calculate that the maximum power factor ($S^2\sigma$) was $1.45 \times 10^{-3} \text{ W}/\text{m}^2\text{K}^2$ for n-GaAs with doping concentration of $1 \times 10^{17} \text{ cm}^{-3}$. Refer to the thermal conductivity data reported by S. Hava and R. Hunsperger^[8], we could calculate the figure of merit, $ZT = S^2 \sigma / k$ ^[5]. With the known ZT, we could estimate the maximum cooling temperature of this material in the ideal

situation by the equation, $T_{\text{max}} = \frac{1}{2} ZT_c^2$ ^[9]. Thus, we find

out that the material that Berger et. al. worked on could only achieve a maximum cooling temperature of 3.3°C at ideal situation, when considering the contact resistance and other non-ideal factors, the maximum cooling will be further diminished.

Recently, the InP-based superlattice microcooler experimentally demonstrated maximum cooling up to 2.5°C with cooling power density $\sim 100 \text{ W}/\text{cm}^2$ at room temperature

[10,11,12] The enhanced cooling power density was achieved by adding a few μms of superlattice layer (InGaAs/InGaAsP). Superlattice could reduce cross-plane thermal conductivity lower than alloys due to the increased phonon scattering [13]. Furthermore, the superlattice layer acts as an energy filter in the thermionic emission process, thus enhancing the hot electrons filtering. Jizhi Zhang et. al. [14] also fabricated $\text{Al}_{0.1}\text{Ga}_{0.9}\text{As}/\text{Al}_{0.2}\text{Ga}_{0.8}\text{As}$ n-type superlattice microrefrigerators, which cools 0.8°C at 25°C and 2°C at 100°C for a $60 \times 60 \mu\text{m}^2$ device. No cooling power density results reported on their devices. All these results demonstrated a promising trend in the thermoelectric field by introducing the low-dimensional confinement structure as superlattice, quantum dots etc [15].

In this paper, we will discuss the maximum cooling and cooling power densities of InGaAs/InAlAs superlattice microrefrigerators including non-ideal factors and propose an optimized structure to improve the cooling, at the same time, we will also propose two possible integration solutions, monolithic growth, and two-chip flip-chip bonding. A 3D electrothermal models using ANSYSTM [16] was used to evaluate the preliminary results.

2. Device Structure and 3D electrothermal model

The heterostructure-integrated thermionic (HIT) microrefrigerator consists of a superlattice layer $\text{In}_{0.53}\text{Ga}_{0.47}\text{As}/\text{Al}_{0.52}\text{Ga}_{0.48}\text{As}$, lattice matched to an n+-InP substrate ($330 \mu\text{m}$ -thick), and a $0.3 \mu\text{m}$ -thick InGaAs layer highly doped ($1 \times 10^{19} \text{cm}^{-3}$) InGaAs used as buffer layer and cap layer for top and bottom contacts. The superlattice contained 25 periods of 5nm thick InGaAs n-doped with doping concentration of $3 \times 10^{19} \text{cm}^{-3}$ and 3nm thick undoped InAlAs. The whole structure was grown using molecular beam epitaxy (MBE). Devices were fabricated using conventional lithography, dry etching and metallization techniques. Ni/AuGe/Ni/Au was used to make ohmic contacts to both electrodes. Figure 1 shows a schematic cross-section view of the device. Figure 2 shows the device structure with fine meshing in a 3D electrothermal model.

In our ANSYSTM model, bulk Joule heating and heat conduction are automatically calculated by solving current continuity and heat conduction equations. We treat the thermionic emission cooling process as interface cooling/heating effects, which were calculated in a linear transport region by $\Delta Q = (S_1 - S_2) \cdot T \cdot I$ at both the metal-superlattice and superlattice-substrate interfaces. S_1 and S_2 are the effective Seebeck coefficients for materials on the two sides of the junctions: for the metal-superlattice interface, $S_1 = S_{\text{metal}}$, $S_2 = S_{\text{superlattice}}$; for the superlattice-substrate interface, $S_1 = S_{\text{superlattice}}$, $S_2 = S_{\text{si}}$. T is the ambient temperature and I the supplied current. Table 1. lists material properties that we used in the simulation. The cross-plan thermal conductivity of the superlattice was measured by Prof. Majumdar's group at UC Berkeley [17]. The Seebeck coefficient data was also experimentally measured. [18] A detailed description of the 3D electrothermal model could be found in reference. [19]

There are two methods we could use to integrate the microrefrigerators with optoelectronic devices. One is to monolithically grow the optoelectronic module on top of the microrefrigerator, which could benefit all the cooling that a single microrefrigerator could create. The second method is to flip-chip bond the optoelectronic module and microrefrigerator together, which we called the two-chip integration model (illustrated in Figure 3). In our model, we create a microrefrigerator chip and a $600 \times 400 \mu\text{m}^2$ optoelectronic chip. We flip-chip bond the two modules together with a $3 \mu\text{m}$ gold interface and a $0.3 \mu\text{m}$ SiN_x insulating layer. At the target-cooling area, the optoelectronic device's active region, we apply heat flux to simulate the heating generated by an optoelectronic device's active region. For convenient calculation, we make the heat flux size equal to the microrefrigerator device size.

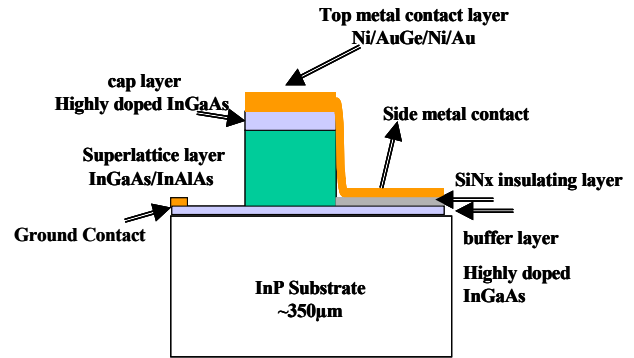


Figure 1 A cross-section view of the device geometry (drawing not to scale for best illustration only)

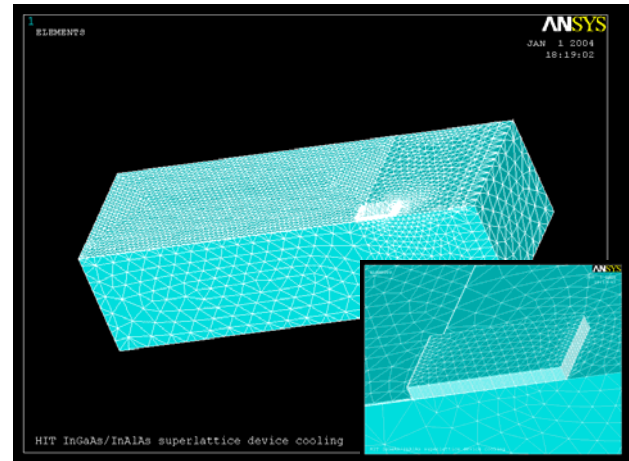


Figure 2 HIT microcooler with fine meshing in a 3D electrothermal model, right corner enlarged picture to illustrate the fine meshing in superlattice region

Thermal Conductivity						
Unit	Metal layer	SiNx	InP Substrate	Bottom Contact layer	SL Layer	Top Contact Layer
W/mK	72	1	68	6.7	6.7	6.7
Resistivity						
Ohm-cm	1.00e-05	1000	0.006	0.001	0.001	0.031

Table 1 Materials parameters for InGaA/InAlAs superlattice microrefrigerator

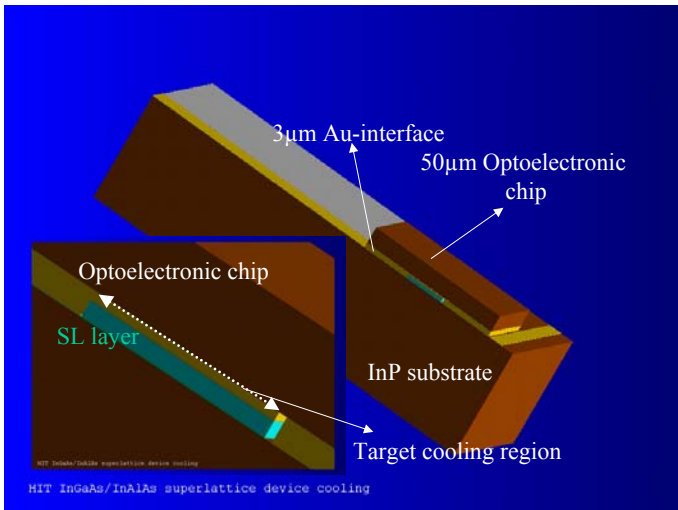


Figure 3 The two-chip integration model of microrefrigerator with optoelectronic module

3. Maximum cooling and cooling power density

The performance of the microrefrigerator was evaluated in terms of maximum cooling temperature and cooling power density in all experiments and simulations below.

The maximum cooling we discuss in this paper refers to the temperature difference between the microrefrigerator top surface (T_c) and the heatsink (T_s) ($\Delta T = T_s - T_c$). To verify the simulation model, the maximum cooling for various device sizes were also experimentally measured with two Omega™ E-type thermocouples, one on top of the microrefrigerator, and the other on top of the InP substrate, which was placed on the temperature controlled copper stage with thermal grease.

The cooling power was defined as the heat that the microrefrigerator could take at the point maximum cooling equals to zero. The cooling power density equals the cooling power divide by the device area.

4. Results and discussion

4.1. Current device cooling (simulation vs. experiments)

In Figure 4, we could see a good correspondence between the simulation and experiment, which ensures the accuracy of the model. Furthermore, we also investigated cooling power densities of these devices with the current model, as

illustrated in Figure 5. For current experimental devices, we could expect a cooling power density ranging from 25 W/cm² to 135 W/cm² for device size, 40x40µm² to 120x120µm².

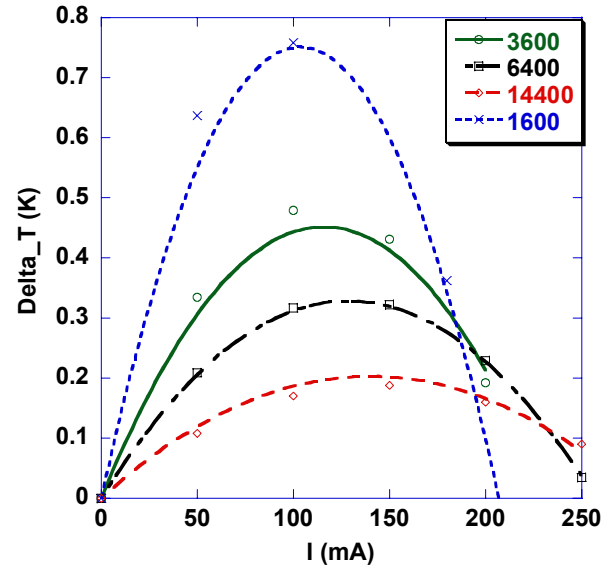


Figure 4 Experimental versus simulated cooling for various device sizes (individual dots are experimental measurement results, curves are simulated results)

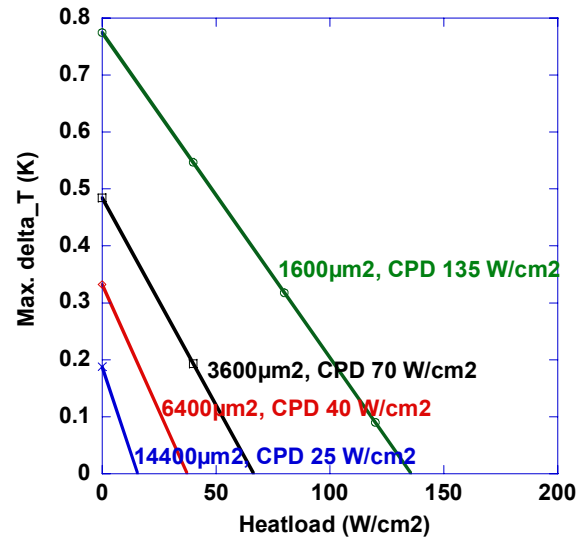


Figure 5 Simulated maximum cooling temperature versus applied heatflux for various device sizes, and cooling power densities (CPD) are also given in the graph

4.2. Improved device cooling

From Figure 4 and Figure 5, we found out that the cooling of the device is very limited, ~0.8°C though the cooling power density is over 100 W/cm². From the simple calculations that we mentioned in the introduction part, we knew that the maximum capacity of these devices would be in the order of 3~4°C. Obviously, the non-ideal factors greatly diminish the maximum cooling of the device. We could use the 3D electrothermal model and optimize the structure to reduce these non-idealities.

First, we study the superlattice thickness and we find that thicker superlattices have higher cooling. Figure 6 illustrates the maximum cooling that we could achieve if we increase the superlattice thickness to 10 μm and keep all the other parameters the same. The maximum cooling of devices increases two times over the current device.

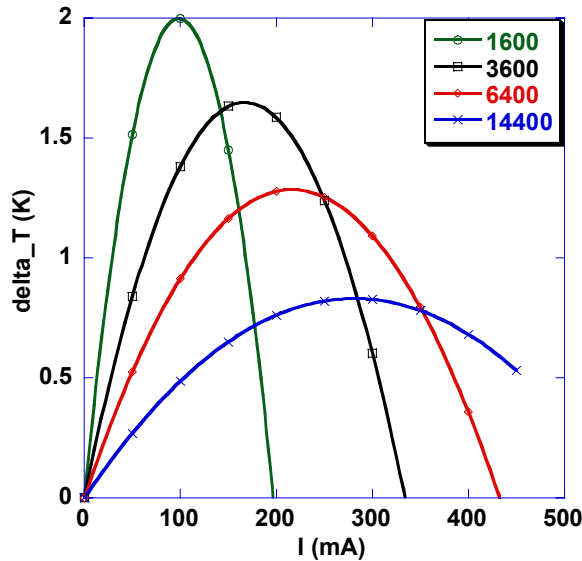


Figure 6 Improved (base on Figure 4 results) maximum cooling with increased 10 μm -thick superlattice layer

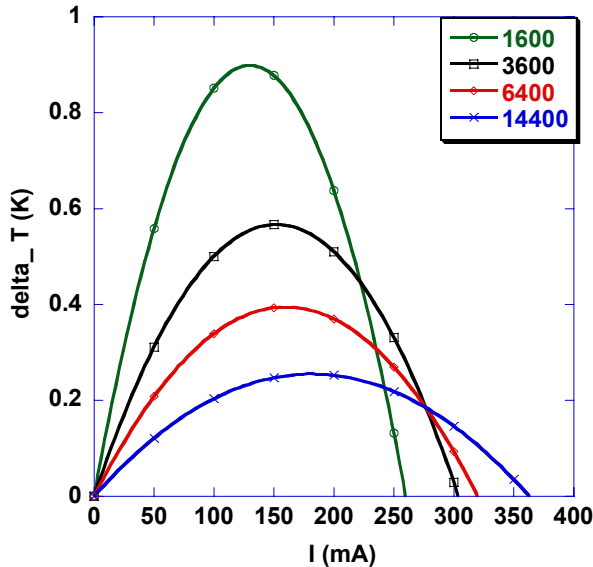


Figure 7 Slightly improved (base on Figure 4 results) maximum cooling with reduced metal/semiconductor contact resistance

Second, we investigate the parasitic influence of metal-semiconductor contact resistance. From the experience of Si/SiGe superlattice microrefrigerator devices, we know this contact resistance is the bottleneck. For the Si/SiGe superlattice microrefrigerator, reducing this contact resistance, the maximum cooling of microrefrigerator could be doubled (from 4.5 $^{\circ}\text{C}$ to 9 $^{\circ}\text{C}$) [19]. It is interesting to find out that reducing the metal-semiconductor contact resistance from

1e-6 ohm-cm 2 to 1e-8 ohm-cm 2 for this device only improves cooling by ~10% as illustrated in Figure 7.

Third, we also check the side contact resistance influence on the microrefrigerator cooling by reducing the side contact resistance to one tenth of its original value. Since the side contact resistance and its thermal conductivity was constrained by Wiedemann-Franz law, process conditions and material properties, the changing range is very limited. When we decrease the electrical resistivity, we had to increase the thermal conductivity at the same time. Thus it generates less Joule heating but the heat is easier to superimpose on top of microrefrigerator cooling region. From Figure 8, we found that the side contact resistance does not improve the cooling for small devices but it almost double the cooling for larger device, as 120x120 μm^2 . It might because the contact probe is larger for large devices.

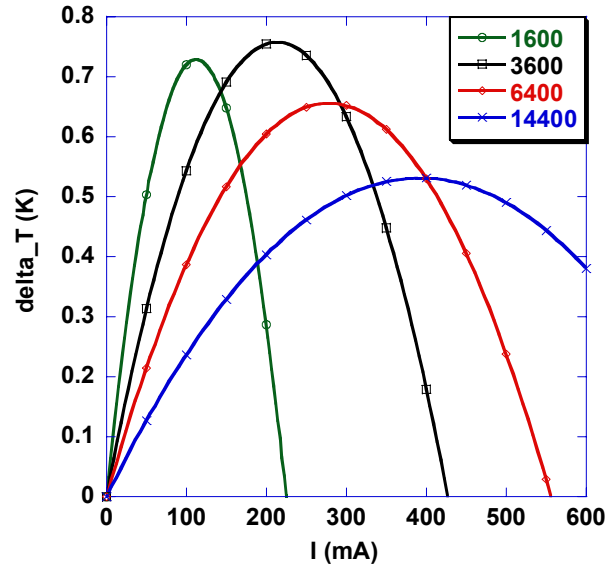


Figure 8 Improved (base on Figure 4 results) cooling with reduced side contact metal resistance

When we put the above three factors together, thicker superlattice, lowering metal contact resistance and lowering side contact resistance, the overall optimized cooling effect is illustrated in Figure 9. We made these three changes since we know that these improvements could be achieved by improving the superlattice growth technique and device fabrication processes. With these improvements, the maximum cooling could achieve 3 $^{\circ}\text{C}$ for device 40x40 μm^2 and 1.5 $^{\circ}\text{C}$ for 120x120 μm^2 device, which is close to the theoretical limit, 4 $^{\circ}\text{C}$, which we calculated from

$$T_{\max} = \frac{1}{2} ZT_c^2 \text{ for this material. Besides the improvement on}$$

maximum cooling temperature, the cooling power densities also increase significantly. The large cooling power density makes it promising for hotspot cooling, removing the hot spots from very small local area and spreading them into the big substrate. Figure 10 illustrates the simulated cooling power density of all device sizes of this optimized device as compared with the original experimental devices. As we could see, the maximum cooling power density is increased three times for the larger device 120x120 μm^2 but less than

two times increment for the small device size $40 \times 40 \mu\text{m}^2$. This non-monotonic change will be further investigated in future work.

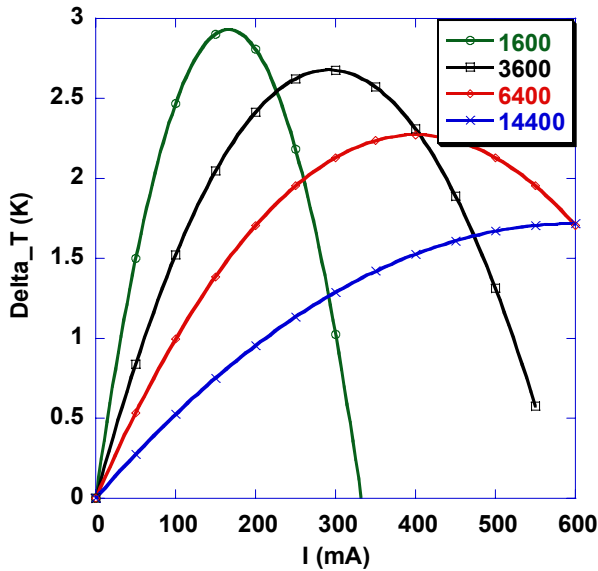


Figure 9 Improved cooling with higher superlattice layer ($10 \mu\text{m}$), reduced metal/semiconductor contact resistance and reduced side metal contact resistance

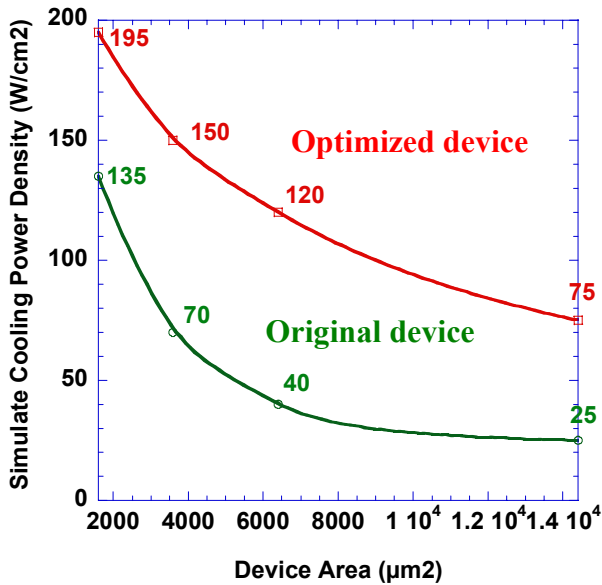


Figure 10 Simulated cooling power densities versus device sizes for optimized superlattice devices as compared with the current experimental devices

Another parasitic non-ideal factor that we could consider is the Joule heating from the substrate. Figure 11 illustrates the maximum cooling that we could achieve if we remove the InP substrate and put the superlattice device directly on a copper plate. We noted that by removing the substrate, the cooling improvement for a larger size device is more significant than smaller devices. As illustrated in Figure 11, Zhang, Superlattice Microrefrigerators Flip-Chip Bonded ...

the $120 \times 120 \mu\text{m}^2$ device will have comparable cooling to the small device, like $40 \times 40 \mu\text{m}^2$. The optimized device size is also increased to $60 \times 60 \mu\text{m}^2$ with a maximum cooling $\sim 4^\circ\text{C}$. However, it requires more electrical power to reach the maximum cooling. For example, the largest device $120 \times 120 \mu\text{m}^2$ requires 1.6A to reach its maximum cooling 3.5°C as compared with 0.6A to reach 1.5°C with substrate. These are all the factors that we need to consider while optimizing the device and applying them to hotspots. Actually if we prefer monolithic growth laser structure directly on top of microrefrigerator, we still need keep the InP-substrate.

However, all the results presented above are not the limit capability of heterostructure integrated thermionic microrefrigerator. According to the recent simulation result [20,21], we could improve the device power factor five times if we could introduce the non-conserved lateral momentum with a higher doping in the superlattice layer. This could be achieved by growing quantum dot layers at the superlattice interface layers. If we include this power factor improvement in our 3D electrothermal model, it is interesting to find out that the small size $40 \times 40 \mu\text{m}^2$ microrefrigerator could cool up to 14°C with a cooling power density exceeding 900 W/cm^2 ; even the largest device $120 \times 120 \mu\text{m}^2$ could achieve a maximum cooling of 6°C with cooling power density of 275 W/cm^2 , as illustrated in Figure 12 and Figure 13. It is important to note that such significant cooling power density is achieved with less than 1A current, which makes it a highly efficient microrefrigerator and promising candidate for optoelectric device cooling.

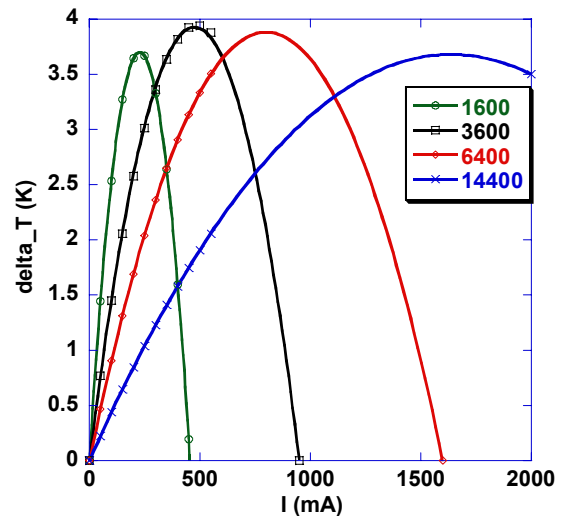


Figure 11 Improved cooling by removing InP substrate (improvements based on Figure 9 results)

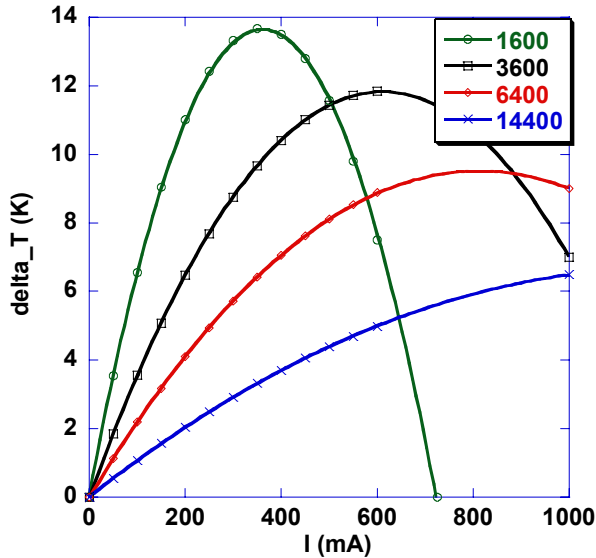


Figure 12 Improved cooling with non-conserved lateral momentum in the superlattice layer and with higher doping (improvements based on Figure 9 results)

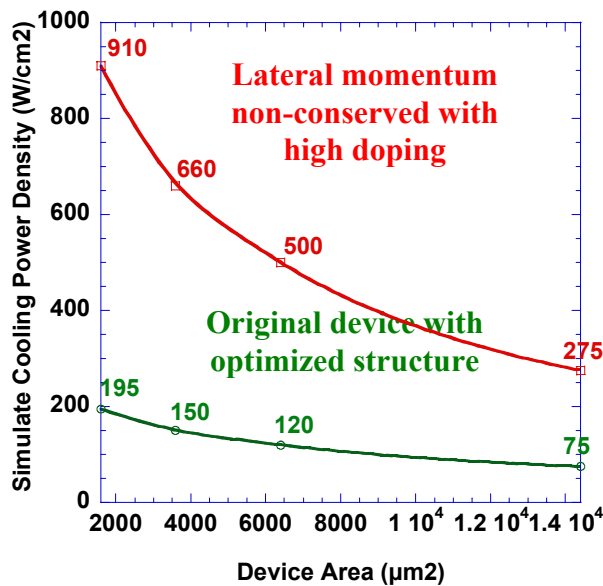


Figure 13 Improved cooling power densities versus device sizes with non-conserved lateral momentum as compared with the optimized device in Figure 9

4.3. Two-chip Integration model simulation results

All above sections discussed the cooling effects that we could achieve if we monolithically grow the laser structure directly on top of the microrefrigerator and if the current could uniformly applied to the cooler device^[22]. However, monolithic integration might be complicated when considering all the growth conditions. Another easy option to utilize the microrefrigerator is to directly flip-chip bond the optoelectronic chip on top of the microrefrigerator as two-chip integrated model. We did a preliminary evaluation based on our current device geometry and integration model

illustrated in Figure 3. This model might not be the optimized structure, which is used as a concept demonstration. From the maximum cooling and cooling power density results in Figure 14 and Figure 15, we noticed that most of the cooling has been lost in the interface layer. The optimized device model had a maximum cooling of 3⁰C, however, it only cools 0.4⁰C after integrating with the optoelectronic module. It is also noted that after it is integrated with optoelectronic module, larger devices cool better at the target-cooling region than the smaller ones. This is opposite to the trend for individual microrefrigerators. The great loss also reflects on the cooling power density reduction. For the optimized structure, the cooling power density reduces to ~50 W/cm² compared to the 200 W/cm² without optoelectronic module, which means only one quarter of the cooling power is used effectively to cool our targeted cooling region. We could improve the cooling power density to 910 W/cm² for non-conserved lateral momentum superlattice samples, but this only provide 300W/cm² at the target region in the flip-chip bonded module, where only one-third of the power is utilized. When we flip-chip bond the microrefrigerator with the optoelectronic devices, there are many system issues we need to address. At this point, the low COP (or ZT of the material) is not the main limiting factor. The more important is the additional thermal resistance due to the integration of microrefrigerators. A more complete system level analysis on integration Si/SiGe superlattice microrefrigerator with microprocessors is studied in an upcoming paper.^[23] At the same time, another point worth mentioning here is the definition of ΔT : in our paper, for the convenience of experimental measurements, we refer ΔT as the microrefrigerator cooling ΔT lower than ambient, normally, on an operating die, ΔT refers to the temperature difference turn on and off the refrigerator. Through simulations^[23], we found out the definition of ΔT lower than ambient actually underestimates ~30% of its cooling capability on the operating die.

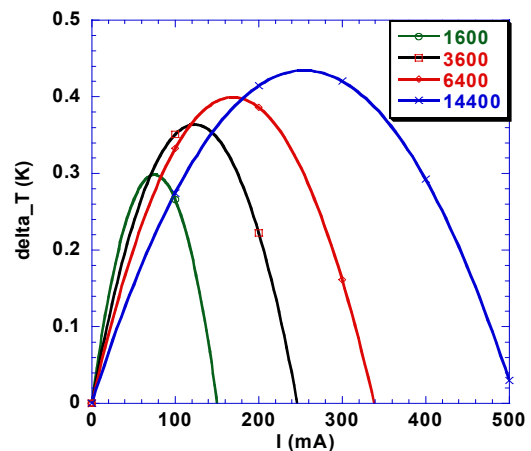


Figure 14 Simulated cooling at targeted cooling region in integrated model with optimized device with maximum cooling illustrated in Figure 9

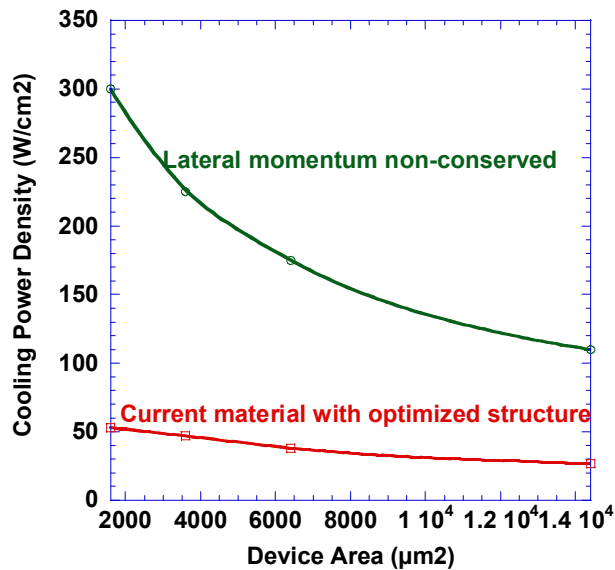


Figure 15 Simulated cooling power densities versus device sizes for optimized device structure (Figure 9) as compared with non-conserved lateral momentum superlattice structure (Figure 12)

5. Conclusions

We built up a 3D electrothermal model to simulate the InP-based InGaAs/GaAlAs superlattice microrefrigerator using ANSYS finite element analysis method. We analyzed the non-ideal factors, including metal/semiconductor contact resistance, side contact resistance, and substrate Joule heating. The original-designed device could experimentally achieve a maximum cooling of $\sim 0.8^\circ\text{C}$ with a cooling power density of 135 W/cm^2 . The optimized device structure could achieve a maximum cooling of 3°C with a cooling power density of 195 W/cm^2 , with an increased superlattice height to $10\mu\text{m}$, reduced metal/semiconductor contact resistance, and reduced side contact resistance. Furthermore, if we could introduce non-conserved lateral momentum in the superlattice structure with the use of embedded quantum dots, the device could demonstrate a maximum cooling of 14°C with a cooling power density of 910 W/cm^2 . If we monolithically grow the optoelectronic device on top of these microrefrigerators, this maximum cooling could be achieved. However, when we use two-chip flip-chip bonded integration model, the interface materials have been the bottleneck limiting the microrefrigerators ability to cool the target hotspots on optoelectronic module. With the current $3\mu\text{m}$ Au-interface together with $0.3\mu\text{m}$ - SiN_x insulating layer interface, only one-fourth to one-third of the cooling power could reach the hotspots, 50 W/cm^2 with the current optimized superlattice structure and 300 W/cm^2 for lateral momentum non-conserved superlattice structure. How to efficiently integrate the microrefrigerator chips with the optoelectronic module will be next step research primary task.

Acknowledgments

This work was supported by DRAPA HERETIC and NSF CAREER.

References

1. Yan Zhang, James Christofferson, Daryoosh Vashaee, Phuong Nguyen, Gehong Zeng, Chris LaBounty, Yae Okuno, Yi-Chen Chiu, John Bowers and Ali Shakouri, "Thin film coolers for localized temperature control in optoelectronic integrated circuits", Proceedings of 53rd Electronic components and technology conference (ECTC), 2003, New Orleans, LA, P312
2. H. B. Sequeira, "Thermoelectric properties of a Peltier cooled laser structure" Ph.D. dissertation, University of Delaware, Newark, DE, 1982
3. Yan Zhang, James Christofferson and Ali Shakouri, Gehong Zeng, John Bowers and Ed Croke "High Speed Localized Cooling using SiGe Superlattice Microrefrigerators", 19th Annual IEEE Semiconductor Thermal Measurement and Management Symposium, San Jose, CA, Mar., 2003, P61
4. Shlomo Hava, Robert G. Hunsperger and H. Brian Sequeira, "Monolithically Peltier-Cooled Laser Diodes", Journal of Lightwave Technology, Vol. LT-2, No. 2 April, 1984, P175
5. N. K. Dutta, T. Cella, R. L. Brown, and D. T. C. Huo, "Monolithically integrated thermoelectric controlled laser diode", Applied Physics Letters 47 (3) August, 1985, P222
6. Paul R. Berger, Niloy K. Dutta, Kent D. Choquette, Ghulam Hasnain, and Naresh Chand, "Monolithically Peltier-cooled vertically-cavity surface-emitting lasers", Applied Physics Letters, 59 (1), July, 1991, P117
7. Chris LaBounty, Ali Shakouri, Patrick Abraham, and John E. Bowers, "Two stage monolithic thin film coolers", ITherm 2000 Conference Proceedings, Las Vegas, NV, May 2000
8. S. Hava and R. Hunsperger, "Thermoelectric properties of $\text{Ga}_{1-x}\text{Al}_x\text{As}$ ", Journal of Applied Physics, 57 (12), June 1985, P5330
9. D. M. Rowe, CRC Handbook of Thermoelectrics, CRC, New York, 1995
10. Christopher LaBounty, Ali Shakouri, Patrick Abraham and John Bowers, "Monolithic integration of thin-film coolers with optoelectronic devices",
11. Yan Zhang, and Ali Shakouri et. al. "Thin film coolers for localized temperature control in optoelectronic integrated circuits" 53rd Electronic Components and Technology Conference proceedings ECTC 2003, New Orleans, May, 27-30th, 2003, P312
12. Christopher LaBounty, Adil Karim, Xiaofeng Fan, Gehong Zeng, Patrick Abraham, Yae Okuno, J. E. Bowers, James, Christofferson, Daryoosh Vashaee, Alberto Fitting, Ali Shakouri, and Edward Croke, "Wafer-fused thin film cooler semiconductor laser structures", 20th, ICT, June, 2001, P397
13. Bao Yang and Gang Chen, "Partially coherent phonon heat conduction in superlattices", Physical Review B, 67, 195311, 2003,

14. JiZhi Zhang, Neal G. Anderson and Kei May Lau, "AlGaAs superlattice microcoolers", *Applied Physics Letters*, 83 (2), July, 2003, P374
15. G. Chen, M.S. Dresselhaus, G. Dresselhaus, J.-P. Fleurial and T. Caillat, "Recent developments in thermoelectric materials", *International Materials Reviews*, 2003 Vol. 48 No. 1
16. ANSYS Release No. 7.0 (2003), ANSYS Inc. Canonsburg, PA
17. Scott T. Huxtable, Chris LaBounty, Ali Shakouri, Patrick Abraham, Yi-Jen Chiu, Xiaofeng Fan, John E. Bowers, and Arun Majumdar, "Thermal conductivity of InP-based superlattices", *Microscale Thermophysical Engineering*, Vol.4, No. 3, 2000.
18. Zhang, Y., Zeng, G., Singh, R., Christofferson, J., Croke, E., Bowers, J. E., and Shakouri, A., "Measurement of Seebeck coefficient perpendicular to SiGe superlattice", 21st ICT, August, 2002, Long Beach
19. Yan Zhang, Daryoosh Vashaee, James Christofferson, Gehong Zeng, Chris LaBounty, J. Piprek, Ed Croke and Ali Shakouri et. al. "3D electrothermal simulation of heterostructure thin film microcooler" 2003 ASME Symposium on the Analysis and Applications of Heat Pump & Refrigeration Systems Proceeding, Nov.16th – 21st, 2003, Washington, DC
20. Yan Zhang, Daryoosh Vashaee, Rajeev Singh, Gehong Zeng and Ali Shakouri, "Influence of Doping Concentration and Ambient Temperature on the Cross-Plane Seebeck Coefficient of InGaAs/InAlAs superlattices", to be published in MRS 2003 thermoelectric Proceeding, Boston, MA, 2003.
21. D. Vashaee and A. Shakouri, "Improved thermoelectric power factor in metallic-based superlattices", accepted for publication *physical review letters*, December, 2003
22. Chris LaBounty, David Oberle, Joachim Piprek, Patrick Abraham, Ali Shakouri and John E. Bowers, "Monolithic integration of solid state thermionic coolers with semiconductor lasers", *Laser and Electro Optics Society Annual Meeting (LEOS)*, Porto Rico, November 2000.
23. Gary L. Solbrekken, Yan Zhang, Avram Bar-Cohen, and Ali Shakouri, "Use of Superlattice Thermionic Emission for "Hot Spot" Reduction in a Convectively-Cooled Chip", to be published in *Itherm* April 2004